ADVANCED THEORY AND SIMULATIONS
www.advtheorysimul.com

Modeling Hydrogen and Oxygen Evolution Reactions on Single Atom Catalysts with Density Functional Theory: Role of the Functional

*Ilaria Barlocco, Luis A. Cipriano, Giovanni Di Liberto, and Gianfranco Pacchioni**

The most widely used approach to predict catalytic activity is density functional theory, whose results however depend on the adopted exchange-correlation functional. In this work, the role played by the functional in predicting the activity of single atom catalysts (SAC) in the hydrogen and oxygen evolution reactions (HER and OER) is studied. 16 transition metal (TM) atoms embedded in N-doped graphene are simulated and the performance of the widely adopted Perdew–Burke–Ernzerhof (PBE) functional against the hybrid PBE0 functional is assessed. The PBE+*U* approach, a computationally less complex way to correct for the self-interaction error in density functional theory, is also considered. The predictions obtained with PBE have a substantial deviation from PBE0 for first row TMs, i.e., 3d systems, while smaller deviations are found for the 4d and 5d series. The PBE+*U* results represent an improvement with respect to PBE, although some differences from PBE0 remain. This study underlines the importance of the choice of the DFT functional in screening new catalysts and in predicting catalytic activities. The use of PBE appears acceptable for 4d and 5d metals, while in the case of 3d systems PBE+*U* or PBE0 approaches are recommended, in particular for magnetic ground states.

1. Introduction

Electrochemical water splitting is one of the most relevant chemical processes that can contribute to solve the formidable issues related to the generation of clean and sustainable fuels. The process involves the conversion of water molecules into molecular oxygen and hydrogen. The hydrogen evolution reaction (HER) occurs at the cathode of the system ($2H^+ + 2e^- \rightarrow H_2$) and the oxygen evolution reaction (OER) at the anode ($2H_2O \rightarrow O_2 + 4H^+ + 4e^-$).[1–3] The reaction is endergonic with a cost of 4.92 eV for each molecule of oxygen released[4,5] and it is often catalyzed by noble metals, such as Pt.[6,7] The last aspect is critical in terms of sustainability of the process, given the problematic issues of critical raw materials.[8] For this reason, research is intensively dedicated to the development of catalytic material requiring smaller amounts of precious metals and lower overpotentials.

Single-atom catalysts (SACs) can address both aspects.[9–12] SACs consist of isolated metal atoms stabilized on a support, maximizing the exposed active sites. Moreover, their behavior is better defined than supported metal nanoparticles, strongly depending on the surrounding of the single atom[13] and showing behaviors that are reminiscent of coordination compounds,[9,14] allowing in principle to engineer and tailor the catalytic activity in a desired way.

Given the intrinsic atomistic nature of SACs, computational chemistry can be of help to predict, understand and rationalize the behavior of these species. The state-of-the-art methodology relies mostly on density functional theory (DFT) since this approach represents a good compromise between accuracy and computational effort. In this respect, DFT is used nowadays for the screening of large sets of materials for both HER and OER.[14–18] It should be mentioned, however, that validations of this choice based on systematic comparisons of different methods are scarce.

The prediction of reaction energies requires a significant accuracy of the modeling techniques, a nontrivial aspect within DFT.[19,20] In fact, the results depend critically on the choice of the exchange-correlation (XC) functional adopted. The most popular class of functionals is based on the generalized gradient approximation (GGA). One of the most famous parameterizations of this type is the Perdew–Burke–Ernzerhof (PBE),[21] widely adopted for the treatment of SACs. It is curious that this functional has been widely adopted in the study of the chemistry of SACs and that the examples of validation of the PBE functional for this class of systems are rare.[22,23] For instance, in a study of Ag_1 and Cu_1 adatoms on $Fe_3O_4(001)$ it has been shown that hybrid functional-based calculations accurately predict the experimental geometry, while DFT+*U* approaches perform poorly.[24] It is well known

I. Barlocco, L. A. Cipriano, G. Di Liberto, G. Pacchioni
Dipartimento di Scienza dei Materiali
Università di Milano–Bicocca
via R. Cozzi 55, Milano 20125, Italy
E-mail: gianfranco.pacchioni@unimib.it

The ORCID identification number(s) for the author(s) of this article can be found under https://doi.org/10.1002/adts.202200513

DOI: 10.1002/adts.202200513

that generalized gradient approximation (GGA) functionals, including PBE, are affected by the self-interaction error and lead to underestimation of semiconductors band gap and important uncertainties in reaction barriers and energies. This problem is well known, and a way proposed 30 years ago by Becke to solve this issue was to add a fraction of the exact Fock exchange to the DFT functional,[25–28] giving raise to the family of hybrid functionals. Related to the PBE formulation,[29] Adamo and Barone in 1999 proposed the PBE0 model, a hybrid functional containing 25% of exact Fock exchange.[30–35] The improved accuracy of hybrid functionals has a cost in terms of increased computational effort required. On another hand, a more pragmatic approach that does not imply a relevant computational effort is the DFT+U approach, where an on-site Coulomb interaction term (U) between electrons is introduced.[36,37] However, the choice of the "best" U value is not trivial. In general, the choice is done empirically by fitting some quantity of interest. In some cases it possible to adopt well-grounded methodologies.[38]

Given the increase of computational power and the development of artificial intelligence techniques, several studies are based on the screening of hypothetical catalysts at the level of DFT with the PBE functional. In this work we investigate the performance of PBE on a set of SACs and we compare this with the PBE+U and the PBE0 functionals. Several other formulations of the XC functional have been proposed, but PBE0 remains one of the more robust.[39] The data set is made by 16 transition metal atoms, i.e., TM = from Cr to Cu; from Mo to Ag; from W to Au (Re was not included since we encountered convergence problems, while Tc is radioactive and unstable). The TM atoms were embedded in a nitrogen doped graphene, a widely studied support for SACs.[40–46] The results show that, in many cases, the predictions for the HER and OER reactions obtained with the PBE functional present a substantial deviation from those computed at the PBE0 level. This is true in particular for light transition metals, while for the heaviest ones the adoption of PBE looks reasonable. The picture can be improved with DFT+U.

The purpose of this study is thus to alert theorist interested in the prediction of the new single atom catalysts of the importance of properly choosing the exchange-correlation functional, in particular when dealing with TM atoms at the right of the first TM row. While the adoption of the standard PBE functional looks fine for some 4d and 5d TM atoms, a PBE+U approach is recommended when the use of more well-grounded hybrid functionals is not possible due to the dimensions and number of systems to investigate.

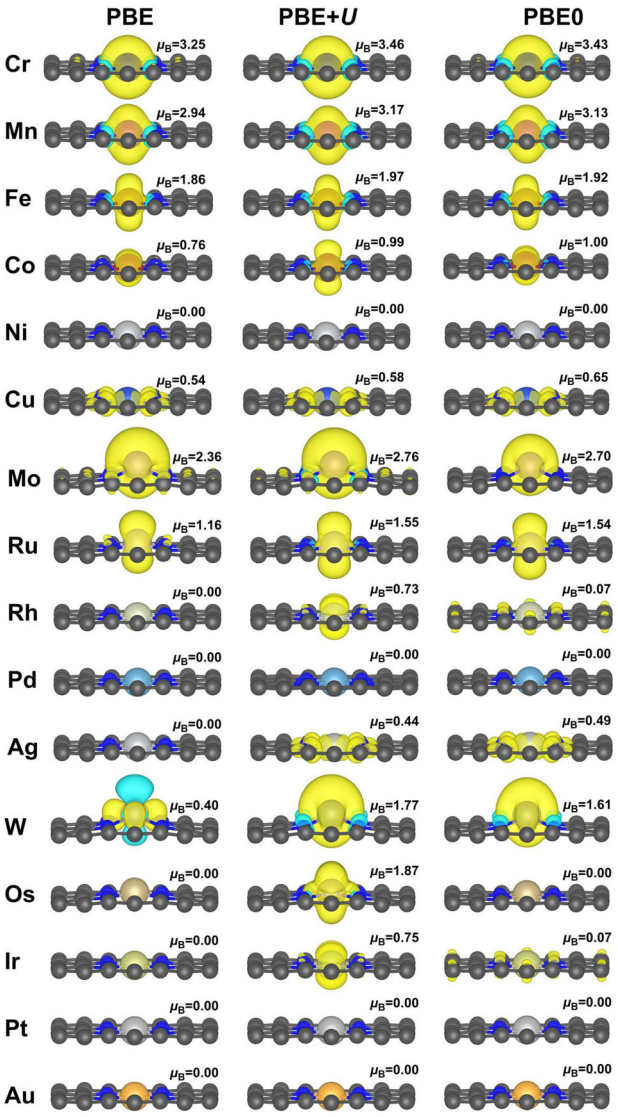

Figure 1. Spin density plot ($\Delta\rho$) of TM supported on N-doped graphene at the different levels of theory. Differences in spin polarization are reported in yellow and blue (iso-surface equal to 5×10^{-3} eÅ^{-3}).

2. Results and Discussion

2.1. H Adsorption on TM@4N-Gr

We first compare the electronic structure of the TM atoms adsorbed in nitrogen-doped graphene (4N-Gr) by looking at the spin-density and the atomic magnetizations (μ_B). **Figure 1** shows the different magnetizations of the TMs considered with PBE, PBE+U and PBE0. In most cases PBE deviates significantly from the PBE0 results, providing more delocalized solutions. This is particularly evident for Co@4N-Gr, Ag@4N-Gr, and W@4N-Gr, Figure 1. This is not surprising, given the well-known problem of charge delocalization of GGA functionals. However, a proper treatment of spin localization is important and it depends on the level of treatment (in particular, in hybrid functionals it depends on the amount of exact Fock exchange).[47] Next we investigated the performance of PBE+U. Most of the PBE+U values of the first two periods are in good agreement with those observed with PBE0 (mean absolute error, MAE = 0.06 μ_B), with the only exception of Rh@4N-Gr. In the case of 5d TMs there are substantial deviations in the case of Os@4N-Gr and Ir@4N-Gr.

The different magnetization of Rh, Os and Ir at PBE+U and PBE0 levels shown in Figure 1 is due to the existence of various electronic configurations with different spin but very similar energies. However, once a H atom is adsorbed, **Table 1**, the near degeneracy of the electronic states is removed and the same magnetization is found at the PBE+U and PBE0 levels. In particular, for the TM-H complexes Co, Rh, Ir all show the same zero net

Table 1. Gibbs energy of H on single TM atom supported on N-doped graphene at different levels of theory. In all cases, dispersion is included and the reported magnetization value is after hydrogen adsorption.

	ΔG_H [eV]			TM magnetization			
TM-H	PBE	PBE+U	PBE0	PBE	PBE+U	PBE0	U
Cr@4N-Gr	0.32	0.65	0.67	2.64	2.92	2.88	2.93
Mn@4N-Gr	0.53	0.99	1.02	2.17	2.41	2.30	3.06
Fe@4N-Gr	0.37	1.02	1.05	0.94	1.18	1.15	3.29
Co@4N-Gr	0.13	0.60	0.57	0.00	0.00	0.00	3.42
Ni@4N-Gr	1.65	1.61	1.79	0.40	0.91	1.05	3.40
Cu@4N-Gr	1.71	1.95	2.31	2.31	0.66	0.65	4.18
Mo@4N-Gr	−0.41	−0.14	−0.03	1.64	2.12	1.22	2.30
Ru@4N-Gr	−0.47	−0.16	−0.26	0.04	0.79	0.80	2.79
Rh@4N-Gr	−0.24	−0.29	−0.59	0.00	0.00	0.00	3.04
Pd@4N-Gr	1.88	2.00	2.17	0.09	0.15	0.19	3.33
Ag@4N-Gr	0.78	0.79	0.79	0.00	0.00	0.00	3.57
W@4N-Gr	−1.05	−0.76	−0.84	0.91	1.05	1.00	2.08
Os@4N-Gr	−0.62	−0.51	−0.71	0.58	0.89	0.79	2.51
Ir@4N-Gr	−0.35	−0.40	−0.74	0.00	0.00	0.00	2.74
Pt@4N-Gr	1.54	1.58	1.98	0.00	0.00	0.03	2.95
Au@4N-Gr	2.17	2.19	2.31	0.09	0.08	0.09	3.17

magnetization while Fe, Ru and Os, with one electron less, exhibit a net magnetization close to 1, Table 1.

The screening of promising good catalysts for HER is largely based on the Nørskov approach,[48] where the formation of an intermediate made by an adsorbed hydrogen atom (MH) on the catalytic site is considered. This approach was originally proposed for extended metal surfaces, obtaining an impressive success. Indeed, in this case it is possible to use the Gibbs energy of the MH intermediate, ΔG_H, as a unique descriptor for the catalytic activity.[49] In particular, a ΔG_H close to zero corresponds to an active catalyst (top of the volcano plot) while very positive or very negative ΔG_H values correspond to inactive catalysts that bind hydrogen too weakly or too strongly, respectively. This approach was transferred without change to the study of SACs in recent years. However, there are many important aspects that one should account for a reliable prediction of SACs chemical activities, such as the formation of other intermediates (on SACs dihydrogen complexes can also form, HMH[14]), the overpotential,[50,51] and solvation effects.[52] Here, we focus on a primary aspect of the simulation: the impact of the DFT functional adopted on the predicted activity of SACs.[22] Notice that we are not interested here in the definition of the best catalysts, but only in the assessment of the role of the functional. For this reason, effects related to other intermediates, solvent and external potentials are not included.

We limited our evaluation of the Gibbs energy of MH intermediates using the working equation adopted by Nørskov and coworkers,[48] where the entropic contribution of solid-state species is neglected, the entropy of gas phase H_2 at 298 K is taken as 0.40 eV, and the zero-point energy correction term is approximated to 0.04 eV[48]

$$\Delta G_H = \Delta E_H + 0.24 \text{ eV} \quad (1)$$

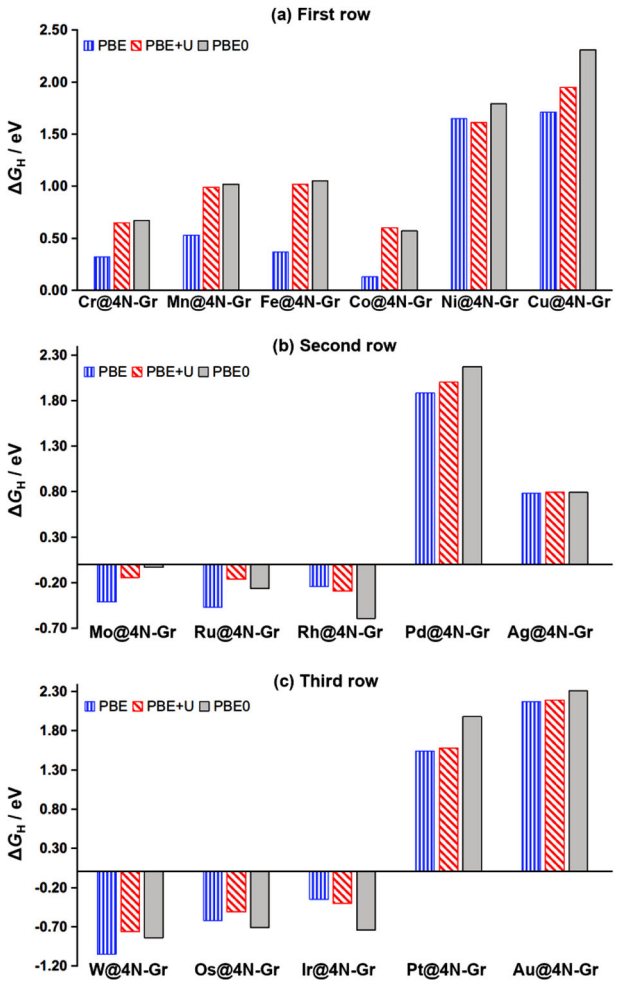

Figure 2. Gibbs energy of hydrogen adsorbed on SACs at different levels of theory.

Given the very large range of calculated ΔG_H values, these approximations can be considered acceptable and, in any case, do not affect the conclusions.

A hydrogen atom was adsorbed on the different SACs and the Gibbs energy was obtained by applying Equation (1) (ΔG_H), Table 1. The magnetic moment of the TM after hydrogen adsorption is also reported in Table 1.

Setting PBE0 as a benchmark, the PBE estimates of the Gibbs energy are often rather different, particularly for 3d and 4d TMs, with an MAE = 0.36 eV. However, the computed Gibbs energies with the PBE+U approach are in much better agreement in most of the cases, MAE = 0.12 eV. The highest deviation is found for Cu@4N-Gr and Rh@4N-Gr (**Figure 2**a,b) where the differences are of 0.39 eV and 0.30 eV, respectively. To underline the importance of the chosen XC functional, one can observe that at the PBE level Cr, Fe, and Co are predicted to be good catalysts for HER (ΔG_H is 0.32, 0.37, 0.13 eV, respectively), while the picture changes if one considers the free energy computed with the PBE0 functional, where the three systems are predicted to be rather inactive (ΔG_H = 0.67, 1.05, 0.57 eV, respectively).

Table 2. Magnetic moment of TM supported on N-doped graphene at different U values.

Catalyst						
U [eV]	0.0	1.0	2.0	3.00	4.0	5.0
			TM magnetization			
Mn@4N-Gr	2.94	3.02	3.10	3.17	3.24	3.37
Fe@4N-Gr	1.86	1.91	1.95	1.97	1.98	1.99

Table 3. Gibbs free energy of H adsorption on Mn and Fe atoms supported on N-doped graphene at different U values. The magnetization values reported refer to the complex with adsorbed H.

U [eV]	0.0	1.0	2.0	3.0	4.0	5.0
ΔG_H [eV]						
Mn@4N-Gr	0.57	0.64	0.81	0.98	1.14	1.30
Fe@4N-Gr	0.33	0.55	0.76	0.96	1.16	1.36
TM magnetization						
Mn@4N-Gr	2.17	2.26	2.34	2.41	2.45	2.47
Fe@4N-Gr	0.94	1.04	1.12	1.16	1.23	1.31

A different trend is found for the 5d TMs, where the results obtained with the PBE functional look more reasonable (MAE = 0.25 eV). In this case, the highest deviation is observed for Ir@4N-Gr, 0.39 eV, which however once more corresponds to go from an active catalyst, ΔG_H(PBE) = −0.35 eV, to an inactive one, ΔG_H(PBE0) = −0.74 eV (Table 1, and Figure 2c).

2.2. Role of the *U* Parameter: Mn@4N-Gr and Fe@4N-Gr

The choice of the U parameter in DFT+U calculations is a delicate issue.[19,53] Therefore, we decided to analyze the effect of this term in the specific case of the prediction of HER for two representative cases, Mn@4N-Gr and Fe@4N-Gr. We chose these two systems because they present unpaired electrons both before and after H atom adsorption. We sampled the U values ranging from U = 0 eV, corresponding to a standard PBE calculation, to U = 5 eV, a rather high value. We observe from **Table 2** that increasing U results in the enhancement of the metal magnetization, as expected.

Next, the Gibbs energies of hydrogen adsorption have been computed for different U values, **Table 3**. A linear correlation between U and ΔG_H is obtained (**Figure 3**), indicating that increasing U implies a less favorable (more endergonic) interaction between hydrogen and TM@4N-Gr. Figure 3 shows that the choice of U is critical, since by tuning the value of U one can go from a very small ΔG_H (strong interaction) to a very large one (weak interaction). This is an aspect that should be critically considered when DFT+U is adopted to predict the activity of SACs. We also observe that the ΔG_H values obtained with U parameters taken from Ref. [54] are in good agreement with the PBE0 results (Figure 2a), providing a validation for the adoption of these U values.

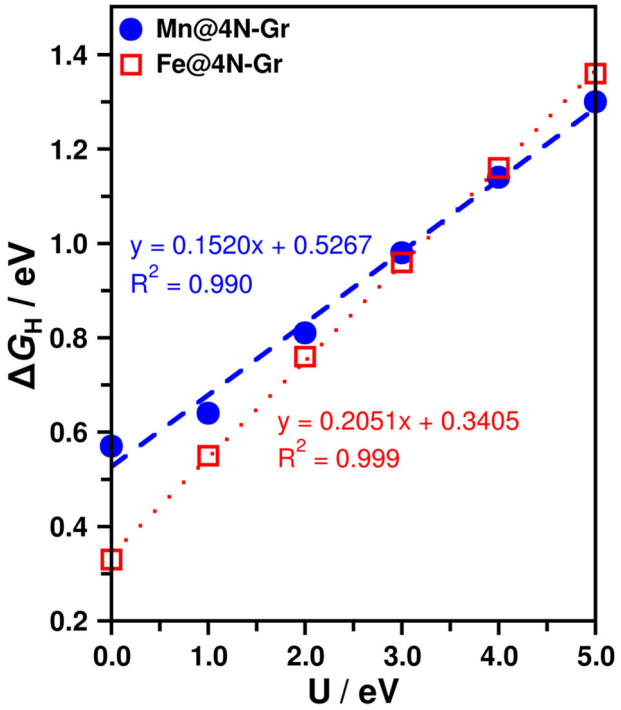

Figure 3. Gibbs energy of hydrogen adsorbed on Mn@4N-Gr and Fe@4N-Gr as a function of the U parameter.

2.3. Oxygen Evolution Reaction on TM@4N-Gr

In the previous section we showed that the use of different functionals can have a strong effect on the calculated ΔG_H and the predicted catalytic activity in HER. We now consider the OER but we restrict the analysis to four representative cases, i.e., Mn@4N-Gr, Fe@4N-Gr, Co@4N-Gr, and Ni@4N-Gr, and we evaluate the effect of the functional on the predicted activities. Once more, these catalysts are chosen for their importance in this kind of reactions and because they present large differences in HER depending on the functional adopted.

We model OER according to the well-known path occurring on metals that implies the formation of OH*, O*, and OOH* intermediates (the active site is labeled with *)

$$* + H_2O \rightarrow OH^* + H^+ + e^- \quad (2)$$

$$OH^* \rightarrow O^* + H^+ + e^- \quad (3)$$

$$O^* + H_2O \rightarrow OOH^* + H^+ + e^- \quad (4)$$

$$OOH^* \rightarrow O_2 + H^+ + e^- \quad (5)$$

The related equations to compute the Gibbs energy of each intermediate are reported in Section S1 (Supporting Information). The calculated Gibbs energies of the intermediates are reported in **Table 4**, assuming to apply a voltage V = 1.23 V. The modeling of OER is clearly more complicated given the higher number of species involved. In this scenario, we observe again how fundamental, and impacting is the choice of the DFT functional. Starting from the first intermediate, OH*, Table 4 and **Figure 4**a,

Table 4. Gibbs energy of OH*, O*, and OOH* intermediates on single TM atoms supported on N-doped graphene at different levels of theory. In all cases dispersion is included and the magnetization value is after the intermediate adsorption.

	ΔG [eV] OER (V = 1.23 eV)			TM magnetization		
OH*	**PBE**	**PBE+U**	**PBE0**	**PBE**	**PBE+U**	**PBE0**
Mn@4N-Gr	−0.60	−0.21	−0.12	2.34	2.01	1.89
Fe@4N-Gr	−0.56	0.06	0.21	1.05	1.25	1.10
Co@4N-Gr	−0.15	0.20	0.31	0.00	0.00	0.00
Ni@4N-Gr	0.87	0.93	1.24	0.37	0.46	0.45
O*	**PBE**	**PBE+U**	**PBE0**	**PBE**	**PBE+U**	**PBE0**
Mn@4N-Gr	−1.41	−0.54	−0.03	-0.48	2.62	0.84
Fe@4N-Gr	−0.97	−0.18	0.15	1.22	1.51	1.39
Co@4N-Gr	0.18	0.24	0.59	1.90	2.40	2.49
Ni@4N-Gr	1.59	1.58	2.12	−1.59	1.66	−1.39
OOH*	**PBE**	**PBE+U**	**PBE0**	**PBE**	**PBE+U**	**PBE0**
Mn@4N-Gr	0.14	0.20	1.00	2.03	3.53	1.94
Fe@4N-Gr	0.05	0.77	1.14	2.03	1.17	1.08
Co@4N-Gr	0.64	0.89	1.32	0.29	1.41	0.00
Ni@4N-Gr	1.31	1.38	1.84	0.26	0.25	0.23

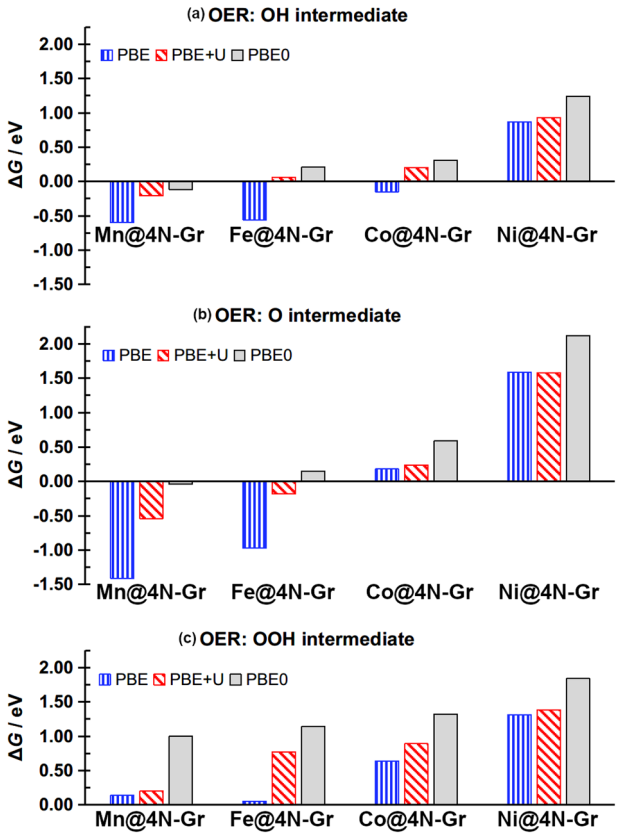

Figure 4. Gibbs free energy of OH*, O*, and OOH* intermediates adsorbed on SACs at different level of theory (V = 1.23 V).

for most of the TMs considered the Gibbs energy obtained at the PBE+U level resembles the PBE0 ones (MAE = 0.17 eV; the only deviation is Ni@4N-Gr where the two values are 0.93 eV and 1.24 eV, respectively). On the contrary, the adoption of the PBE approach implies significant deviations, MAE = 0.52 eV. Particularly relevant is the case of Mn@4N-Gr, where ΔG_H(PBE) = −0.60 eV corresponds to a poor catalyst, while ΔG_H(PBE0) = −0.12 eV indicates an excellent one.

When we move to the second intermediate, O*, the adoption of PBE implies an even higher deviation from PBE0: the MAE is very high, 0.86 eV, and the maximum deviation reaches 1.38 eV, Table 4. It is clear that the two DFT approaches lead to completely different predictions. The picture improves when working with PBE+U, since the mean deviation decreases to 0.43 eV. However, some differences remain, as for the case of Mn@4N-Gr (ΔG_H(PBE+U) = −0.54 eV, ΔG_H(PBE0) = −0.03 eV, Table 4). The situation is consistent even when looking at the last intermediate, OOH*, although the performances of PBE+U are not as good as for other systems. The average deviation is 0.79 eV when working with PBE, and 0.52 eV with PBE+U. Large discrepancies with the PBE0 functional remain (once more, Mn@4N-Gr is a critical case).

This brief discussion demonstrates the critical role played by the choice of the functional in describing the performance of a SAC in OER.

3. Computational Details

Spin polarized DFT calculations were performed with the VASP[55–57] code. We used the Perdew–Burke–Ernzerhof (PBE)[21] and the PBE0[29,34] formulations of the exchange-correlation functional. The PBE+U approach[36,58] has been adopted as well, taking the Hubbard's U terms from the Literature. More specifically, we considered the values reported by Anisimov,[54] and already adopted to study SACs (see Table 1 for the values and the discussion in ref. [23]). Dispersion forces have been included according to the Grimme's D3 parameterization.[59] The following valence electrons were treated explicitly: H (1s), C (2s,2p), N (2s, 2p), O (2s, 2p), Cr (3p, 4s, 3d), Mn (3p, 4s, 3d), Fe (4s, 3d), Co (4s, 3d), Ni (4s, 3d), Cu (4s, 3d), Mo (4p, 5s, 4d), Ru (4p, 5s, 4d), Rh (4p, 5s, 4d), Pd (5s, 4d), Ag (5s, 4d), W (6s, 5p, 5d), Os (6s, 5d), Ir (6s, 5d), Pt (6s, 5d), and Au (6s, 5d). They have been expanded on a set of plane waves with a kinetic energy cutoff of 400 eV, whereas the core electrons were treated with the projector augmented wave approach (PAW).[60,61] The threshold criteria for electronic and ionic loops were set to 10^{-6} eV and 10^{-3} eV/Å, respectively. A 5×5×1 Monkhorst–Pack k-point grid[62] was used to sample the reciprocal space when working with the PBE and PBE+U functionals, and it was reduced to 2×2×1 when the PBE0 was adopted because of the large computational effort required by hybrid functionals.

First, a 4×4×1 supercell of graphene was created considering the pristine graphene lattice parameters ($a = b$ = 2.468 Å, and γ = 120°). The supercell was fully optimized with the three functionals. A vacuum layer of 15 Å was added in each calculation to avoid spurious effects due to interaction between periodic replica of the system along the non-periodic direction. The optimized lattice parameters are: $a = b$ = 9.870 Å, γ = 120°,[23,63] and $a = b$ = 9.811

Å, $\gamma = 120°$ for PBE and PBE0 functionals, respectively. Then, we created a pyridinic defect by generating a C divacancy and replacing four C atoms with N atoms. The TM atoms were embedded in this coordination site, giving rise to the TM@4N-Gr systems. The atomic coordinates were always fully relaxed keeping the lattice constants fixed to those of graphene. We have shown in fact that the optimization of the lattice constants for each TM atom incorporated in the doped graphene layer has very little effect of the total energies.[23]

4. Conclusions

In this work we studied the impact of three different DFT functionals on the prediction of the catalytic activity of SACs consisting of TM atoms embedded in nitrogen-doped graphene in two relevant reactions, the HER and the OER. We assessed the performance of PBE, which is commonly adopted to study the activity of SACs, the PBE0 hybrid functional, and PBE+*U* approach often used to study semiconducting materials but more rarely adopted in the study of SACs. We simulated a set of 16 transition metal atoms (from Cr to Cu; from Mo to Ag; from W to Au, with the exception of Re and Tc). Regarding HER, the calculation of the Gibbs free energies for HER and OER indicate that, taking PBE0 as a reference, the predictions of PBE are often substantially deviating from the results of the hybrid functional. This is particularly true for some 3d, while the error is smaller for 4d and 5d elements. In fact, the mean average deviation is largest for the first TM series, MAE = 0.45 eV (3d), compared to the second and third raw of TM atoms, MAE = 0.25 eV (4d) and 0.25 eV (5d). Notice that there is not only a quantitative problem in reproducing the Gibbs free energies, but also a qualitative difference, with some SACs that are predicted to be very active at the PBE level and totally inactive using the PBE0 hybrid functional. Considering the large number of screening studies to predict new SACs appeared in the literature which are entirely based on DFT-PBE or similar functionals, this is an important warning.

The picture can be improved by adopting the PBE+*U* approach, since the deviation (MAE) becomes acceptable and decreases to 0.11 eV, 0.14 eV, 0.23 eV for 3d, 4d, and 5d metals respectively. The overall deviation is 0.15 eV, to be compared with MAE = 0.33 eV of the PBE results. Once more, the average deviation is not so relevant as the analysis of the individual cases: for instance, Fe@4N-Gr is predicted to be a good HER catalyst at the PBE level ($\Delta G_H = 0.37$ eV) and a very poor catalyst at the PBE+U level ($\Delta G_H = 1.02$ eV). Similar conclusions have been obtained on the OER. Here we selected a representative set of 3d metals finding that PBE significantly deviates from PBE0, while the adoption of the PBE+*U* approach mitigates the problem. It is interesting to note that the *U* values adopted in this work have been derived for TM atoms embedded in a Ru metal,[54] while here we are dealing with TMs formally in positive oxidation state. It remains to be investigated if *U* values specifically derived for different atomic configurations can further improve the DFT+*U* results.

The main message of this study is thus that more attention should be given to the adopted functional in computational studies of the activity of SACs. We have shown that the results may critically depend on this choice. While for some atoms using a standard GGA functional such as PBE is not so critical, e.g., for some 5d elements, the treatment of SACs with magnetic ground states and in particular with localized d electrons, as for atoms at the right of the first TM raw, can lead to completely wrong conclusions.

Supporting Information

Supporting Information is available from the Wiley Online Library or from the author.

Acknowledgements

The authors acknowledge the financial support from the Cariplo Foundation through the project "Carbon dioxide conversion into energy-rich molecules with tailored catalysts" (CO2ENRICH). Access to the CINECA supercomputing resources was granted via ISCRAB. The authors also thank the COST Action 18234 supported by COST (European Cooperation in Science and Technology).

Open access Funding provided by Universita degli Studi di Milano-Bicocca within the CRUI-CARE Agreement.

Conflict of Interest

The authors declare no conflict of interest.

Data Availability Statement

The data that support the findings of this study are available from the corresponding author upon reasonable request.

Keywords

DFT, functionals, HER, OER, SACs

Received: July 18, 2022
Revised: August 11, 2022
Published online: September 4, 2022

[1] J. H. Kim, D. Hansora, P. Sharma, J.-W. Jang, J. S. Lee, *Chem. Soc. Rev.* **2019**, *48*, 1908.
[2] M. G. Walter, E. L. Warren, J. R. McKone, S. W. Boettcher, Q. Mi, E. A. Santori, N. S. Lewis, *Chem. Rev.* **2010**, *110*, 6446.
[3] A. Kudo, Y. Miseki, *Chem. Soc. Rev.* **2009**, *38*, 253.
[4] X. Li, X. Hao, A. Abudula, G. Guan, *J. Mater. Chem. A* **2016**, *4*, 11973.
[5] C. C. L. McCrory, S. Jung, I. M. Ferrer, S. M. Chatman, J. C. Peters, T. F. Jaramillo, *J. Am. Chem. Soc.* **2015**, *137*, 4347.
[6] J. D. Benck, T. R. Hellstern, J. Kibsgaard, P. Chakthranont, T. F. Jaramillo, *ACS Catal.* **2014**, *4*, 3957.
[7] Z. W. Seh, J. Kibsgaard, C. F. Dickens, I. Chorkendorff, J. K. Nørskov, T. F. Jaramillo, *Science* **2017**, *355*, 146.
[8] European Commission, *Critical Raw Materials Resilience: Charting a Path towards Greater Security and Sustainability*, **2020**.
[9] S. J. Gutić, A. S. Dobrota, E. Fako, N. V. Skorodumova, N. López, I. A. Pašti, *Catalysts* **2020**, *10*, 290.
[10] A. Wang, J. Li, T. Zhang, *Nat. Rev. Chem.* **2018**, *2*, 65.
[11] N. Cheng, S. Stambula, D. Wang, M. N. Banis, J. Liu, A. Riese, B. Xiao, R. Li, T.-K. Sham, L.-M. Liu, G. A. Botton, X. Sun, *Nat. Commun.* **2016**, *7*, 13638.

[12] G. Vilé, G. Di Liberto, S. Tosoni, A. Sivo, V. Ruta, M. Nachtegaal, A. H. Clark, S. Agnoli, Y. Zou, A. Savateev, M. Antonietti, G. Pacchioni, *ACS Catal.* **2022**, *12*, 2947.
[13] J. Hulva, M. Meier, R. Bliem, Z. Jakub, F. Kraushofer, M. Schmid, U. Diebold, C. Franchini, G. S. Parkinson, *Science* **2021**, *371*, 375.
[14] G. Di Liberto, L. A. Cipriano, G. Pacchioni, *J. Am. Chem. Soc.* **2021**, *143*, 20431.
[15] H. Xu, D. Cheng, D. Cao, X. C. Zeng, *Nat. Catal.* **2018**, *1*, 339.
[16] Z. Wang, J. Zhao, Q. Cai, F. Li, *J. Mater. Chem. A* **2017**, *5*, 9842.
[17] H.-C. Huang, Y. Zhao, J. Wang, J. Li, J. Chen, Q. Fu, Y.-X. Bu, S.-B. Cheng, *J. Mater. Chem. A* **2020**, *8*, 9202.
[18] L. Li, R. Huang, X. Cao, Y. Wen, *J. Mater. Chem. A* **2020**, *8*, 19319.
[19] G. Pacchioni, *Catal. Lett.* **2015**, *145*, 80.
[20] A. J. Cohen, P. Mori-Sánchez, W. Yang, *Chem. Rev.* **2012**, *112*, 289.
[21] J. P. Perdew, K. Burke, M. Ernzerhof, *Phys. Rev. Lett.* **1996**, *77*, 3865.
[22] A. M. Patel, S. Ringe, S. Siahrostami, M. Bajdich, J. K. Nørskov, A. R. Kulkarni, *J. Phys. Chem. C* **2018**, *122*, 29307.
[23] G. Di Liberto, L. A. Cipriano, G. Pacchioni, *ACS Catal.* **2022**, *12*, 5846.
[24] M. Meier, Z. Jakub, J. Balajka, J. Hulva, R. Bliem, P. K. Thakur, T.-L. Lee, C. Franchini, M. Schmid, U. Diebold, F. Allegretti, D. A. Duncan, G. S. Parkinson, *Nanoscale* **2018**, *10*, 2226.
[25] A. D. Becke, *J. Chem. Phys.* **1992**, *96*, 2155.
[26] A. D. Becke, *J. Chem. Phys.* **1993**, *98*, 1372.
[27] A. D. Becke, *J. Chem. Phys.* **1992**, *97*, 9173.
[28] A. D. Becke, *J. Chem. Phys.* **1996**, *104*, 1040.
[29] J. P. Perdew, M. Ernzerhof, K. Burke, *J. Chem. Phys.* **1996**, *105*, 9982.
[30] L. M. Debefve, C. J. Pollock, *Phys. Chem. Chem. Phys.* **2021**, *23*, 24780.
[31] D. Coskun, S. V. Jerome, R. A. Friesner, *J. Chem. Theory Comput.* **2016**, *12*, 1121.
[32] C. Adamo, V. Barone, *Theor. Chem. Acc.* **2000**, *105*, 169.
[33] C. M. Lousada, P. A. Korzhavyi, *J. Comput. Chem.* **2016**, *37*, 787.
[34] C. Adamo, V. Barone, *J. Chem. Phys.* **1999**, *110*, 6158.
[35] G. Di Liberto, S. Tosoni, G. Pacchioni, *J. Phys. Chem. Lett.* **2019**, *10*, 2372.
[36] S. L. Dudarev, G. A. Botton, S. Y. Savrasov, C. J. Humphreys, A. P. Sutton, *Phys. Rev. B* **1998**, *57*, 1505.
[37] J. Hubbard, B. H. Flowers, *Proc. R. Soc. London, Ser. A* **1964**, *281*, 401.
[38] H. J. Kulik, M. Cococcioni, D. A. Scherlis, N. Marzari, *Phys. Rev. Lett.* **2006**, *97*, 103001.
[39] M. G. Medvedev, I. S. Bushmarinov, J. Sun, J. P. Perdew, K. A. Lyssenko, *Science* **2017**, *355*, 49.
[40] Z. Du, X. Chen, W. Hu, C. Chuang, S. Xie, A. Hu, W. Yan, X. Kong, X. Wu, H. Ji, L.-J. Wan, *J. Am. Chem. Soc.* **2019**, *141*, 3977.
[41] S. Zhou, L. Shang, Y. Zhao, R. Shi, G. I. N. Waterhouse, Y.-C. Huang, L. Zheng, T. Zhang, *Adv. Mater.* **2019**, *31*, 1900509.
[42] V. Fung, G. Hu, Z. Wu, D. Jiang, *J. Phys. Chem. C* **2020**, *124*, 19571.
[43] L. Liu, S. Liu, L. Li, H. Qi, H. Yang, Y. Huang, Z. Wei, L. Li, J. Xu, B. Liu, *J. Mater. Chem. A* **2020**, *8*, 6190.
[44] R. Jayan, M. M. Islam, *J. Phys. Chem. C* **2021**, *125*, 4458.
[45] W. Gong, F. Zhao, L. Kang, *Comput. Theor. Chem.* **2018**, *1130*, 83.
[46] D. Van Dao, L. A. Cipriano, G. Di Liberto, T. T. D. Nguyen, S.-W. Ki, H. Son, G.-C. Kim, K. H. Lee, J.-K. Yang, Y.-T. Yu, G. Pacchioni, I.-H. Lee, *J. Mater. Chem. A* **2021**, *9*, 22810.
[47] M. Gerosa, C. Di Valentin, C. E. Bottani, G. Onida, G. Pacchioni, *J. Chem. Phys.* **2015**, *143*, 111103.
[48] J. K. Nørskov, T. Bligaard, A. Logadottir, J. R. Kitchin, J. G. Chen, S. Pandelov, U. Stimming, *J. Electrochem. Soc.* **2005**, *152*, J23.
[49] J. Greeley, T. F. Jaramillo, J. Bonde, I. Chorkendorff, J. K. Nørskov, *Nat. Mater.* **2006**, *5*, 909.
[50] K. S. Exner, *Int. J. Hydrogen Energy* **2020**, *45*, 27221.
[51] P. Lindgren, G. Kastlunger, A. A. Peterson, *ACS Catal.* **2020**, *10*, 121.
[52] M. T. Tang, X. Liu, Y. Ji, J. K. Norskov, K. Chan, *J. Phys. Chem. C* **2020**, *124*, 28083.
[53] M. Capdevila-Cortada, Z. Łodziana, N. López, *ACS Catal.* **2016**, *6*, 8370.
[54] I. V. Solovyev, P. H. Dederichs, V. I. Anisimov, *Phys. Rev. B* **1994**, *50*, 16861.
[55] G. Kresse, J. Hafner, *Phys. Rev. B* **1993**, *47*, 558.
[56] G. Kresse, J. Hafner, *Phys. Rev. B* **1994**, *49*, 14251.
[57] G. Kresse, J. Furthmüller, *Comput. Mater. Sci.* **1996**, *6*, 15.
[58] A. I. Liechtenstein, V. I. Anisimov, J. Zaanen, *Phys. Rev. B* **1995**, *52*, R5467.
[59] S. Grimme, J. Antony, S. Ehrlich, H. Krieg, *J. Chem. Phys.* **2010**, *132*, 154104.
[60] P. E. Blöchl, *Phys. Rev. B* **1994**, *50*, 17953.
[61] G. Kresse, D. Joubert, *Phys. Rev. B* **1999**, *59*, 1758.
[62] H. J. Monkhorst, J. D. Pack, *Phys. Rev. B* **1976**, *13*, 5188.
[63] G. Di Liberto, L. A. Cipriano, G. Pacchioni, *ChemCatChem* **2022**, https://doi.org/10.1002/cctc.202200611